

$\alpha = 1.2 \alpha = 1.2 \alpha = 1.3 \alpha = 1.3$

# Analysis of psychological drivers sensitivity in lattice hydrodynamics traffic flow model with passing effect

Meenakshi<sup>a</sup>, Poonam Redhu<sup>b</sup>

<sup>a</sup>*Department of Mathematics, Maharshi Dayanand University, Rohtak, 124001, Haryana, India*

<sup>b</sup>*Department of Mathematics, Maharshi Dayanand University, Rohtak, 124001, Haryana, India*

---

## Abstract

In this paper, we studied the effect of psychological headway (PH) with a passing effect in a new lattice model. The effect of psychological headway with passing is examined through linear stability analysis. Using nonlinear stability analysis, we obtained the range of PH with a passing constant for which the kink soliton solution of mKdV equation exists. For smaller values of coefficient of PH and passing effect, uniform flow and kink jam phases are present on the phase diagram and jamming transition occurs between them. The theoretical findings are verified using numerical simulation, which confirms that traffic jams can be suppressed efficiently by considering the psychological headway with passing in the new lattice model.

*Keywords:* Lattice hydrodynamic model, Psychological headway, Passing effect

---

## 1. Introduction

Indeed, traffic jams have become a significant concern over the past decade due to the exponential growth of automobiles on the roads. As urbanization and economic development continue to progress, the number of vehicles has surged, leading to increased traffic congestion in many cities around the world. Traffic congestion not only affects daily commuters but also has broader implications on various aspects of society, including the economy, environment, and public health. To address these challenges, scholars and researchers have been working on various strategies and solutions to alleviate traffic congestion and improve traffic flow. Therefore, a large number of traffic models have been proposed, such as car-following models, macro-traffic models, cellular automaton models, and hydrodynamic lattice models, to explain traffic phenomena as [1, 2, 3, 4, 5, 6, 7, 8, 9]. But the lattice hydrodynamic model is also a good representation to solve traffic

problems, and its variants have been valuable tools in traffic research and also contributed to our understanding of traffic phenomena and the development of traffic management strategies. Our proposed problem is based on this model and it treats traffic flow as a fluid-like phenomenon, applying principles from fluid dynamics to model the movement of vehicles on the road. To characterize the evolution of the jamming transition in traffic flow, Nagatani[10] firstly introduced a lattice model. After that, several extensions have been done by considering various factors as driver's anticipation effect with passing [11], traffic jerk[12], low and high sensitivity of vehicles[13], predictive effect in two-lane[14], area occupancy[15], multi-lane[16], historical current integration effect[17], heterogeneous lane changing rates[18], curved road with passing[19], backward looking and flow integral[20], driver's memory effect[21], connected and non-connected vehicles[22], H-infinity at highway tunnel[23], driver's sensory memory[24], Impact of Strong-Wind and Optimal Estimation of Flux Difference Integral[25], Study on Energy Dissipation and Fuel Consumption[8], four-way pedestrian traffic with turning capacity[26].

When driving in actual traffic, the driver constantly modifies his or her speed in accordance with the surrounding traffic conditions and makes assumptions about how to drive and try to pass the vehicles to see the effect of psychological headway.

Psychological headway refers to the perceived or desired spacing between vehicles that drivers maintain for safety and comfort reasons, rather than the physical headway (actual distance) between vehicles.

The passing effect in traffic theory refers to a phenomenon where a vehicle that overtakes another vehicle can create a disturbance in the traffic flow behind it. This disturbance is often characterized by a temporary reduction in the speed of surrounding vehicles and an increase in traffic density, which can lead to a ripple effect propagating backward through the traffic stream. Psychological headway comes into play when drivers decide how closely they want to follow the vehicle in front of them while considering the possibility of passing. By considering the psychological headway and the passing effect, the lattice hydrodynamics traffic flow model can better capture real-world traffic phenomena, including the propagation of traffic waves, the formation of congestion, and the emergence of passing maneuvers.

Here we investigate the effect of psychological headway with passing effect on the traffic flow. This prompts us to develop a lattice model by incorporating the effect of psychological headway with passing.

The paper is structured into six sections, each covering different aspects of the

research on traffic flow modeling. The sections and their respective contents are as follows: Section 2 introduces a more accurate and varied lattice model for a single lane that incorporates the driver's psychological headway with a passing effect. The suggested model's linear stability analysis is carried out in Section 3. The nonlinear analysis from which the mKdV equation is obtained is covered in Section 4. In Section 5, numerical simulations are performed, and the conclusion is provided in Section 6.

## 2. Model

The basic lattice hydrodynamic model proposed by Nagatani [10] is a modified version of the lattice gas cellular automaton (LGCA) model. It was developed to study the propagation and evolution of density waves in a unidirectional single-lane scenario, such as traffic flow on a single-lane highway. The model equation is described as

$$\rho_j(t + \tau) - \rho_j(t) + \tau \rho_0 [\rho_j(t) v_j(t) - \rho_{j-1}(t) v_{j-1}(t)] = 0 \quad (1)$$

$$\rho_j(t + \tau) v_j(t + \tau) = \rho_0 V(\rho_{j+1}) \quad (2)$$

where  $\rho_j(t)$  and  $v_j(t)$  are the local density and velocity at  $j^{th}$  site on the one-dimensional lattice at time  $t$ , respectively.  $\rho_0$  and  $a = 1/\tau$  respectively, are the average density and the driver's sensitivity.

The optimal velocity function is

$$V(\rho_j(t)) = \frac{V_{max}}{2} \left[ \tanh \left( \frac{1}{\rho_j} - \frac{1}{\rho_c} \right) + \tanh \left( \frac{1}{\rho_c} \right) \right] \quad (3)$$

where  $V_{max}$  and  $\rho_c$  denote the maximal velocity and the safety-critical density, respectively. Adopting the optimal velocity function for the symmetry of density, as given by Bando[] in 1995, implies using a specific mathematical formulation to model the behavior of vehicles in the lattice hydrodynamic model. Bando's optimal velocity function is a crucial component of the model and is designed to achieve symmetry in vehicle density and traffic flow.

Afterwards, many researchers have made significant advancements in the field of lattice hydrodynamic models for traffic flow and have introduced various modifications and considerations to enhance the model's realism and applicability. Some of these developments include [27, 28, 29, 30]

It seems like you are describing a hypothetical scenario involving traffic and drivers attempting to pass slower vehicles in order to maintain their optimal speed. The statement also mentions that passing is proportional to the difference in traffic between two sites. Based on this description, it appears that the drivers are trying to maintain their ideal or desired speed, and when they encounter congestion or slower traffic at a specific site  $j$ , they attempt to pass the vehicles in front of them to regain their desired speed. The extent of passing is determined by the difference between the optimal traffic current at site  $j$  and the traffic current at the subsequent site  $j + 1$ . Small values of passing provide a phase transition from the kink jam to the uniformity area when it is below the critical value, while larger values with enhanced sensitivity produce a phase transition from the kink jam to the free flow region through the chaotic jam zone. Thus, it is evident that passing significantly influences the characteristics of traffic flow. Nagatani [] thereby accounts for the passing effect, and the evolution equation is given as

$$\rho_j(t + \tau)v_j(t + \tau) = \rho_0V(\rho_{j+1}(t)) + \gamma[\rho_0V(\rho_{j+1}(t)) - \rho_0V(\rho_{j+2}(t))] \quad (4)$$

where  $\gamma$  is the passing constant and  $V(\cdot)$  is the optimal velocity function as discussed above.

The above optimal velocity function is monotonically decreasing and has an upper bound and an inflection point at  $\rho = \rho_c = \rho_0$ . Here, passing is purposely assumed to be constant for the sake of simplicity. In the direction of traffic flow with car following models, Jiang et al. [31], by considering the driver's different psychological headway to understand how people make decisions and react while driving, walking, or cycling on the roads and the model equation is

$$\frac{dv_n(t)}{dt} = a[V(\alpha_n \Delta x_n) - v_n(t)] + \lambda \Delta v_n(t) \quad (5)$$

where  $\alpha_n$  is psychological response coefficient.

In order to see the effect of psychological headway with passing, we modified the LH model in which the continuity equation remains intact while the flow evolution equation is modified by the effect of psychological headway and passing. The modified equation is

$$\rho_j(t + \tau)v_j(t + \tau) = \rho_0V(\alpha\rho_{j+1}(t)) + \gamma[\rho_0V(\alpha\rho_{j+1}(t)) - \rho_0V(\alpha\rho_{j+2}(t))] \quad (6)$$

Here  $\alpha$  is the psychological headway.

The updated optimal velocity function is

$$V(\alpha\rho_j(t)) = \frac{V_{max}}{2} \left[ \tanh\left(\frac{1}{\alpha\rho_j} - \frac{1}{\rho_c}\right) + \tanh\left(\frac{1}{\rho_c}\right) \right] \quad (7)$$

The density equation can be obtained by removing the velocity  $v_j$  from equations (1) and (7).

$$\begin{aligned} &\rho_j(t+2\tau) - \rho_j(t+\tau) + \tau\rho_0^2[V(\alpha\rho_{j+1}) - V(\alpha\rho_j)] \\ &- \tau\rho_0^2\gamma[V(\alpha\rho_{j+2}) - 2V(\alpha\rho_{j+1}) + V(\alpha\rho_j)] = 0 \end{aligned} \quad (8)$$

when we take  $\alpha = 1$  then the equation reduces to the one discussed by Nagztani.[].

### 3. Linear Stability Analysis

In this section, we conducted a linear stability analysis to examine the impact of passing and psychological headway on traffic flow. Under uniform traffic circumstances, the optimal velocity and traffic density are considered as  $\rho_0$  and  $V(\alpha\rho_0)$ , respectively. Let's look at the steady-state solution for homogeneous traffic flow.

$$\rho_j(t) = \rho_0 \quad (9)$$

$$V(\alpha\rho_j(t)) = V(\alpha\rho_0) \quad (10)$$

Assume that site- $j$ 's steady-state density is perturbed slightly by  $y_j(t)$ . Then

$$\rho_j(t) = \rho_0 + y_j(t) \quad (11)$$

$$V(\alpha\rho_j(t)) = V(\alpha\rho_0) + V'(\alpha\rho_0)\alpha y_j(t), \quad (12)$$

When  $\rho_j(t) = \rho_0 + y_j(t)$  is substituted into equation (8), we get

$$\begin{aligned} &y_j(t+2\tau) - y_j(t+\tau) + \tau\rho_0^2\alpha V'(\alpha\rho_0)[y_{j+1}(t) - y_j(t)] \\ &- \gamma\tau\rho_0^2\alpha V'(\alpha\rho_0)[y_j(t) - 2y_{j+1}(t) + y_{j+2}(t)] = 0 \end{aligned} \quad (13)$$

where  $V'(\alpha\rho_0) = \frac{dV(\alpha\rho)}{d\rho}$  at  $\rho = \rho_0$

Using the expression  $y_j(t) = e^{ikj+z\tau}$  in equation (13), we get

$$e^{2z\tau} - e^{z\tau} + \tau\rho_0^2\alpha V'(\alpha\rho_0)[e^{ik} - 1] - \gamma\tau\rho_0\alpha V'(\alpha\rho_0)[1 - 2e^{ik} + e^{2ik}] = 0 \quad (14)$$

By adding  $z = z_1(ik) + z_2(ik)^2 \dots$  to equation (15), we obtain

$$\begin{aligned} & 2\tau z_1(ik) - 2\tau z_2(ik)^2 - (\tau^2/2)z_1^2(ik)^2 + 2\tau^2 z_1^2(ik)^2 - \tau z_1(ik) \\ & - \tau z_2(ik)^2 + \tau \rho_0^2 \alpha V'(\alpha \rho_0)(ik) + \tau \rho_0^2 \alpha V'(\alpha \rho_0)((ik)^2/2) \\ & - \gamma \tau \rho_0^2 \alpha V'(\alpha \rho_0)(ik)^2 = 0 \end{aligned} \quad (15)$$

Now, we get the first and second order terms of the coefficients  $ik$  and  $(ik)^2$ , respectively.

$$z_1 = -\rho_0^2 \alpha V'(\alpha \rho_0) \quad (16)$$

$$z_2 = -\frac{3}{2} \tau (\rho_0^2 \alpha V'(\alpha \rho_0))^2 - \frac{(1-2\gamma)}{2} (\rho_0^2 \alpha V'(\alpha \rho_0)) \quad (17)$$

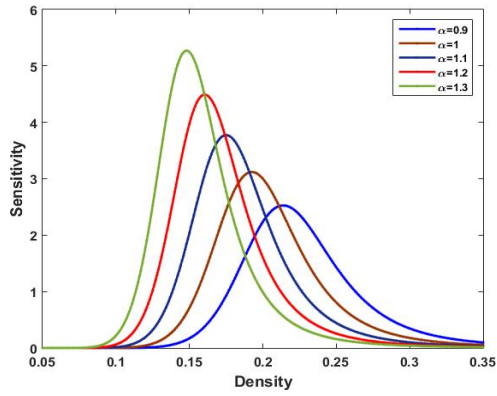
Long-wavelength waves cause the uniform steady-state flow to become unstable when  $z_2 < 0$ . The uniform flow will be maintained as long as  $z_2 > 0$ . As a result, the neutral stability curve is represented by

$$\tau = -\frac{1-2\gamma}{3\rho_0^2 \alpha V'(\alpha \rho_0)} \quad (18)$$

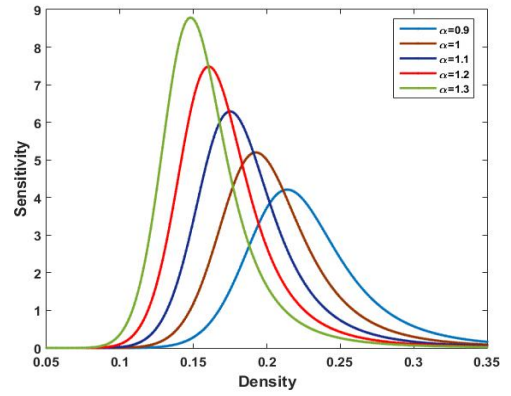
Equation (18) clearly shows that  $\alpha$  and  $\gamma$  play an effective role in stabilizing the traffic flow in maintaining a consistent flow profile to ensure a comfortable psychological headway. Figure 1 shows the neutral stability curves in density-sensitivity space and the apex of each curve indicates the critical point for every value of  $\alpha$ .

In Fig. 1(a) when the passing coefficient is 0.0 (means no passing) it can be easily depicted from the figure that the amplitude of these curves increases with an increase in  $\alpha$  which means that a large value of  $\alpha$  leads to enlargement of an unstable region. Additionally, it is also noted that the value of critical density also changes with a change in the value of  $\alpha$  but overall, the stable region is decreasing.

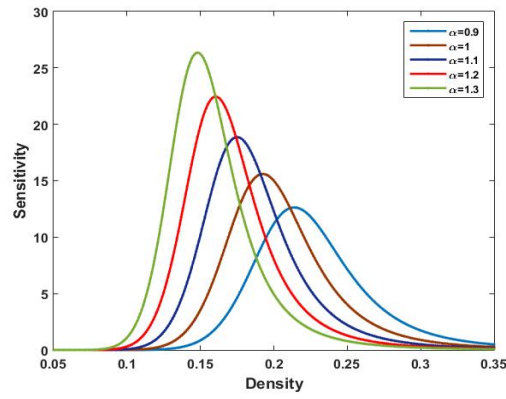
Figure 1(b)-(c) show neutral stability curves in the parameter space  $(\rho_c, a_c)$ . Each curve's peak denotes the critical point, and the stable region exists above neutral curves and the traffic jam does not appear while the unstable region is found below neutral curves and the density wave appears. We take the passing coefficient as 0.2 in Fig.1(b) it can be easily depicted from the figure that the amplitude of these curves increases with an increase in  $\alpha$  which means that a large value of  $\alpha$  leads to enlargement of an unstable region. The behavior is maintained, when we



(a)



(b)



(c)

Figure 1: Phase diagram in density-sensitivity for different value of  $\alpha$  (a)  $\gamma = 0.0$  (b)  $\gamma = 0.2$  (c)  $\gamma = 0.4$

take the passing coefficient as 0.4 in Fig.1(c).

Figure 11(a)-(c) demonstrates that at various values of psychological headway  $\alpha$ , an increase in the value of  $\gamma$  results in an enhancement of the stable region of traffic. The critical points and the neutral stability curves increase with passing constant  $\gamma$ . As psychological headway *alpha* increases, the neutral stability curves also do, but the critical points get decreased. Therefore, by altering the psychological and passing values, one can improve the stability of the transportation system and reduce traffic congestion.

#### 4. Nonlinear

To investigate the nonlinear behavior near the critical point, we used the slower variables  $X$  and  $T$ . Nonlinear analysis allows for the examination of complex interactions between variables that may not be evident in a linear analysis. It can reveal emergent behaviors, stability, instability, and other intricate characteristics that are not apparent in simpler linear models. The analysis focused on a coarse scale, which means they looked at large-scale patterns in the traffic flow. For a small positive parameter  $\varepsilon$ , the slow variables  $X$  and  $T$  are defined as

$$X = \varepsilon(j + bt), T = \varepsilon^3 t \quad (19)$$

where  $b$  is constant to be determined. Let  $\rho_j$  satisfy the following equation:

$$\rho_j(t) = \rho_c + \varepsilon R(X, T) \quad (20)$$

The following nonlinear partial differential equation is obtained by using Eqs. (19) and (20) to expand Eq. (??) up to the fifth order of  $\varepsilon$ :

$$\begin{aligned} \varepsilon^2 k_1 \partial_X R + \varepsilon^3 k_2 \partial_X^2 R + \varepsilon^4 (\partial_T R + k_3 \partial_X^3 R + k_4 \partial_X R^3) + \varepsilon^5 (k_5 \partial_T \partial_X R + k_6 \partial_X^4 R \\ + k_7 \partial_X^2 R^3) = 0 \end{aligned} \quad (21)$$

where the coefficients  $k_i (i = 1, 2, \dots, 7)$  are provided in Table (1), where  $V' = \frac{dV(\rho)}{d\rho}$  and  $V''' = \frac{d^3V(\rho)}{d(\rho^3)}$  at  $\rho = \rho_c$ . In the neighborhood of critical point  $\tau_c$ , we define  $\tau = \tau_c(1 + \varepsilon^2)$  and choosing  $b = -\rho_c^2 \alpha V'(\alpha \rho_c)$ .

Taking  $\varepsilon$ 's second and third order terms out of Eq. (21), we get

$$\varepsilon^4 (\partial_T R - g_1 \partial_X^3 R + g_2 \partial_X R^3) + \varepsilon^5 (g_3 \partial_X^2 R + g_4 \partial_X^4 R + g_5 \partial_X^2 R^3) = 0 \quad (22)$$

Table 1

The coefficients $k_i$ of the model	
$k_1$	$b + \rho_c^2 \alpha V'(\alpha \rho_c)$
$k_2$	$\frac{3}{2} b^2 \tau^2 + \frac{\tau \rho_c^2 \alpha v'(\alpha \rho_c)}{2} - \gamma \tau \rho_c^2 \alpha v'(\alpha \rho_c)$
$k_3$	$\frac{7}{6} b^3 \tau^3 + \frac{\tau \rho_c^2 \alpha v'(\alpha \rho_c)}{6} - \gamma \tau \rho_c^2 \alpha v'(\alpha \rho_c)$
$k_4$	$\frac{\tau \rho_c^2 \alpha^3 v'''(\alpha \rho_c)}{6}$
$k_5$	$3b\tau^2$
$k_6$	$\frac{15}{24} b^4 \tau^4 + \frac{\tau \rho_c^2 \alpha V'(\alpha \rho_c)}{24} - (14) \frac{\gamma \tau \rho_c^2 \alpha V'(\alpha \rho_c)}{24}$
$k_7$	$\frac{\tau \rho_c^2 \alpha^3 v'''(\alpha \rho_c)}{12} - \frac{\gamma \tau \rho_c^2 \alpha^3 v'''(\alpha \rho_c)}{6}$

Table 2

The coefficients $g_i$ of the model	
$g_1$	$-\rho_c^2 \alpha v'(\alpha \rho_c) \left( -\frac{7}{54} (1 - 2\gamma)^2 + \frac{1}{6} - \gamma \right)$
$g_2$	$\frac{\rho_c^2 \alpha^3 v'''(\alpha \rho_c)}{6}$
$g_3$	$-\tau \rho_c^2 \alpha v'(\alpha \rho_c) \left( \frac{1-2\gamma}{2} \right)$
$g_4$	$\rho_c^2 \alpha v'(\alpha \rho_c) \left( \frac{1}{24} \left( \frac{58}{9} \right) (1 - 2\gamma)^3 + \frac{1}{24} (1 - 14\gamma) + \left( \gamma - \frac{1}{6} \right) (1 - 2\gamma) \right)$
$g_5$	$-\frac{\rho_c^2 \alpha^3 v'''(\alpha \rho_c)}{6} \left( \frac{1-2\gamma}{2} \right)$

where Table (2) provides the coefficients  $g_i (i = 1, 2, \dots, 5)$ .

In order to derive the standard mKdV equation, we perform the following transformations in Eq. (22):

$$T' = g_1 T, R = \sqrt{\frac{g_1}{g_2}} R'$$

After implementing the transformation in Eq. (22), we obtain

$$\partial_T R' - \partial_X^3 R' + \partial_X R'^3 + \varepsilon M[R'] = 0, \quad (23)$$

where  $M[R'] = \frac{1}{g_1} \left( g_3 \partial_X^2 R' + \frac{g_1 g_3}{g_2} \partial_X^2 R'^3 + g_4 \partial_X^4 R' \right)$ . We obtain the usual mKdV equation after neglecting the  $O(\varepsilon)$  terms in Eq. (23), whose intended kink soliton solution is given by

$$R'_0(X, T') = \sqrt{c} \tanh \sqrt{\frac{c}{2}} (X - cT'). \quad (24)$$

The solvability condition must be met in order to calculate the propagation velocity for the kink-antikink solution

$$(R'_0, M[R'_0]) \equiv \int_{-\infty}^{\infty} dX R'_0 M[R'_0] = 0, \quad (25)$$

with  $M[R'_0] = M[R']$ . By solving Eq. (25), the value of  $c$  is

$$c = \frac{5g_2g_3}{2g_2g_4 - 3g_1g_5}. \quad (26)$$

Hence, the kink-antikink solution is given by

$$\rho_j(t) = \rho_c + \varepsilon \sqrt{\frac{g_1 c}{g_2}} \tanh \left( \sqrt{\frac{c}{2}} (X - cg_1 T) \right), \quad (27)$$

with  $\varepsilon^2 = \frac{\tau}{\tau_c} - 1$  and the amplitude  $A$  of the solution is

$$A = \sqrt{\frac{g_1}{g_2}} \varepsilon^2 c. \quad (28)$$

Two coexisting phases can be understood by the kink-antikink soliton solution. There is a congested high density phase as well as a low density phase that is free to move, which may be separated from one another using the equation  $\rho_j = \rho_c \pm A$  in the phase space  $(\rho, a)$ .

## 5. Simulation

To evaluate the theoretical findings of the new model's linear and nonlinear analysis with the influence of psychological headway and passing effect, we used numerical simulation. Periodic boundary conditions are established in order to explicitly replicate the proposed model in the stable zone, and the initial condition is determined as

$$\rho_j(0) = \rho_j(1) = \begin{cases} \rho_0 - A, & \text{if } 0 \leq j < \frac{M}{2} \\ \rho_0 + A, & \text{if } \frac{M}{2} \leq j < M \end{cases}$$

Where  $A$  is the initial disturbance and  $M = 100$  is the total number of sites, the relevant parameters are  $\rho_0 = \rho_c = 0.2$ ,  $V_{max} = 2$  and  $A = 0.005$ .

Figure 2 shows the typical density profiles obtained after  $t = 20300$  for  $\gamma = 0.0, 0.2, 0.4$ . The density profiles 2(a)-2(b) show the uniform traffic flow for  $a = 2.8, 2.3$  at  $\gamma = 0.0$  respectively.

Fig.2(a)-(b) the critical points are given as  $\rho_c = 0.213, 0.193$  respectively.

Figure 3 shows the typical density profiles obtained after  $t = 20300$  for  $\gamma = 0.0, 0.2, 0.4$ . The density profiles 3(a)-3(c) show the uniform traffic flow for  $a = 2.8, 3.8, 4.8$  at  $\gamma = 0.0$  respectively.

Fig.3(a)-(c) the critical points are given as  $\rho_c = 0.174, 0.159, 0.149$  respectively.

Fig.3(a)-(c) When  $\gamma = 0.0$ , the fluctuation does not occur for  $\alpha = 1.1, 1.2, 1.3$ , but fluctuation occur for  $\gamma = 0.2, 0.4$ .

The traffic flow 2(a)-(b), 3(a)-(c) obtained after a sufficiently long time is almost uniform spatially but fluctuates a little around  $\rho_0 = 0.2$ .

It is clear from Figs.2(a)-(b) to 3(a)-(c) that the initial uniform perturbation converts into "Kink-antikink density wave" which is the solution of mKdV equation. These density waves propagate in the backward direction as shown in Figs.2-3 and these observations are the same as those that happen in real traffic. It can be observed that an increase in the value of  $\alpha$  corresponds to better stability of traffic flow. It is clear from Figs. ??(a)-(c) that the integration of passing constants for fixed psychological headway plays a significant role in alleviating traffic jams, thus providing empirical validation for the theoretical findings.

These density profiles show distinct traveling waves with varying speeds, which are separated by a growing and decaying density region. The number of stop-and-go waves decreases with a decrease in the coefficients of psychological headway with passing which means that the effect of both factors enhances the stability of the traffic flow.

The amplitude of density waves is weakened with the decrease in the coefficient

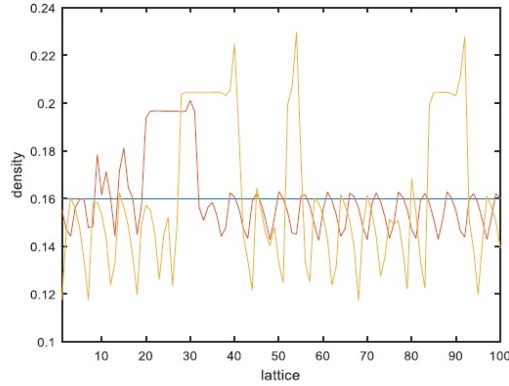


Figure 2: Phase diagram in density-sensitivity for different value of  $\gamma = 0.0, 0.2, 0.4$  at fixed  $\alpha = 0.9$

of psychological headway and passing. The lack of fulfillment of the stability condition leads to the evolution of initial disturbances into a congested flow. Due to the unsatisfied stability condition, the initial disturbances transform into a congested flow.

Moreover, the study shows that when the coefficient of passing is  $\gamma = 0.0$ , the traffic jam completely disappears, and the flow of traffic becomes uniform. This finding emphasizes the importance of implementing efficient traffic control strategies that consider the impact of psychological headway on traffic flow stability. Overall, Fig.2 to Fig.3 provide valuable insights into the dynamics of traffic flow and how it can be stabilized through psychological headway measures. Thus, these simulations underscore the importance of psychological headway and passing effect in influencing traffic stability. It is observed that a larger psychological headway does not effectively alleviate traffic congestion when traffic density is high. However, under low traffic density, a larger psychological headway improves traffic stability and increases traffic flux.

## 6. Conclusion

We investigated the effect of psychological headway (PH) with a passing effect in a new lattice model in this research. The influence of psychological progress on passing is investigated using linear stability analysis. We determined the range of PH with a passing constant for which the kink soliton solution of the mKdV equation exists using nonlinear stability analysis. For lesser values of the coefficient

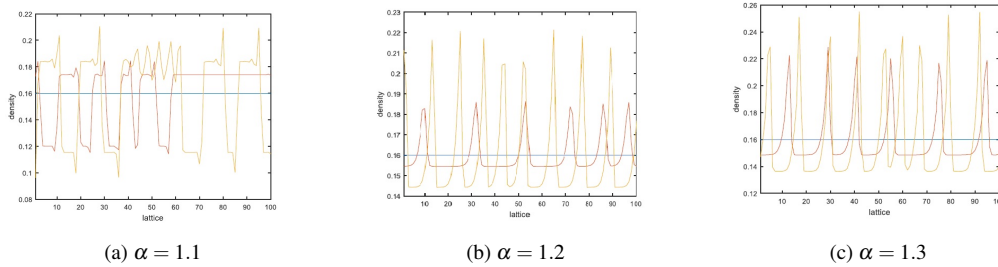


Figure 3: Phase diagram in density-sensitivity for different value of  $\gamma = 0.0, 0.2, 0.4$

of PH and passing effect, the phase diagram shows uniform flow and kink jam phases, with jamming transitions between them. The theoretical conclusions are validated using numerical simulation, which demonstrates that traffic bottlenecks can be effectively alleviated by taking the psychological headway with passing into account in the proposed lattice model.

## References

- [1] M. Bando, K. Hasebe, A. Nakayama, A. Shibata, Y. Sugiyama, Dynamical model of traffic congestion and numerical simulation, *Physical review E* 51 (2) (1995) 1035.
- [2] Y. Li, L. Zhang, S. Peeta, X. He, T. Zheng, Y. Li, A car-following model considering the effect of electronic throttle opening angle under connected environment, *Nonlinear Dynamics* 85 (2016) 2115–2125.
- [3] L. Li, X. M. Chen, Vehicle headway modeling and its inferences in macroscopic/microscopic traffic flow theory: A survey, *Transportation Research Part C: Emerging Technologies* 76 (2017) 170–188.
- [4] Y. Li, H. Zhao, T. Zheng, F. Sun, H. Feng, Non-lane-discipline-based car-following model incorporating the electronic throttle dynamics under connected environment, *Nonlinear Dynamics* 90 (2017) 2345–2358.
- [5] Y. Li, H. Yang, B. Yang, T. Zheng, C. Zhang, An extended continuum model incorporating the electronic throttle dynamics for traffic flow, *Nonlinear Dynamics* 93 (2018) 1923–1931.

- [6] Y. Jiao, R. Cheng, H. Ge, A new continuum model considering driving behaviors and electronic throttle effect on a gradient highway, *Mathematical Problems in Engineering* 2020 (2020) 1–22.
- [7] C. Zhai, W. Wu, S. Luo, Heterogeneous traffic flow modeling with drivers' timid and aggressive characteristics, *Chinese Physics B* 30 (10) (2021) 100507.
- [8] Q. Wen, Y. Xue, B. Cen, Y. Tang, M. Huang, W. Pan, Study on energy dissipation and fuel consumption in lattice hydrodynamic model under traffic control, *Mathematical Problems in Engineering* 2022 (2022).
- [9] S. Yadav, P. Redhu, Driver's attention effect in car-following model with passing under  $v_2v$  environment, *Nonlinear Dynamics* (2023) 1–17.
- [10] T. Nagatani, Modified kdv equation for jamming transition in the continuum models of traffic, *Physica A: Statistical Mechanics and Its Applications* 261 (3-4) (1998) 599–607.
- [11] A. K. Gupta, P. Redhu, Analyses of the driver's anticipation effect in a new lattice hydrodynamic traffic flow model with passing, *Nonlinear Dynamics* 76 (2014) 1001–1011.
- [12] P. Redhu, V. Siwach, An extended lattice model accounting for traffic jerk, *Physica A: Statistical Mechanics and its Applications* 492 (2018) 1473–1480.
- [13] R. Kaur, S. Sharma, Analyses of a heterogeneous lattice hydrodynamic model with low and high-sensitivity vehicles, *Physics Letters A* 382 (22) (2018) 1449–1455.
- [14] D. Kaur, S. Sharma, A new two-lane lattice model by considering predictive effect in traffic flow, *Physica A: Statistical Mechanics and Its Applications* 539 (2020) 122913.
- [15] D. Kaur, S. Sharma, A. K. Gupta, Analyses of lattice hydrodynamic area occupancy model for heterogeneous disorder traffic, *Physica A: Statistical Mechanics and its Applications* 607 (2022) 128184.
- [16] N. Madaan, S. Sharma, A lattice model accounting for multi-lane traffic system, *Physica A: Statistical Mechanics and its Applications* 564 (2021) 125446.

- [17] H. Zhao, G. Zhang, W. Li, T. Gu, D. Zhou, Lattice hydrodynamic modeling of traffic flow with consideration of historical current integration effect, *Physica A: Statistical Mechanics and its Applications* 503 (2018) 1204–1211.
- [18] F. Sun, A. H. Chow, S. Lo, H. Ge, A two-lane lattice hydrodynamic model with heterogeneous lane changing rates, *Physica A: Statistical Mechanics and Its Applications* 511 (2018) 389–400.
- [19] J. Wang, F. Sun, R. Cheng, H. Ge, An extended heterogeneous car-following model with the consideration of the drivers' different psychological headways, *Physica A: Statistical Mechanics and Its Applications* 506 (2018) 1113–1125.
- [20] Q. Wang, H. Ge, An improved lattice hydrodynamic model accounting for the effect of “backward looking” and flow integral, *Physica A: Statistical Mechanics and Its Applications* 513 (2019) 438–446.
- [21] L. Li, R. Cheng, H. Ge, New feedback control for a novel two-dimensional lattice hydrodynamic model considering driver's memory effect, *Physica A: Statistical Mechanics and its Applications* 561 (2021) 125295.
- [22] Y. Zhang, M. Zhao, D. Sun, S. hui Wang, S. Huang, D. Chen, Analysis of mixed traffic with connected and non-connected vehicles based on lattice hydrodynamic model, *Communications in Nonlinear Science and Numerical Simulation* 94 (2021) 105541.
- [23] Y. Zhang, M. Zhao, D. Sun, X. Liu, S. Huang, D. Chen, Robust h-infinity control for connected vehicles in lattice hydrodynamic model at highway tunnel, *Physica A: Statistical Mechanics and its Applications* 603 (2022) 127710.
- [24] Z. Yicai, Z. Min, S. Dihua, Z. Zhaomin, C. Dong, A new feedback control scheme for the lattice hydrodynamic model with drivers' sensory memory, *International Journal of Modern Physics C* 32 (02) (2021) 2150022.
- [25] H. Liu, Y. Wang, Impact of strong wind and optimal estimation of flux difference integral in a lattice hydrodynamic model, *Mathematics* 9 (22) (2021) 2897.

- [26] Y. Tang, Y. Xue, M. Huang, Q. Wen, B. Cen, D. Chen, A lattice hydrodynamic model for four-way pedestrian traffic with turning capacity, *Sustainability* 15 (3) (2023) 2544.
- [27] A. K. Gupta, P. Redhu, Jamming transition of a two-dimensional traffic dynamics with consideration of optimal current difference, *Physics Letters A* 377 (34-36) (2013) 2027–2033.
- [28] P. Redhu, A. K. Gupta, Jamming transitions and the effect of interruption probability in a lattice traffic flow model with passing, *Physica A: Statistical Mechanics And Its Applications* 421 (2015) 249–260.
- [29] P. Redhu, A. K. Gupta, The role of passing in a two-dimensional network, *Nonlinear Dynamics* 86 (2016) 389–399.
- [30] A. K. Gupta, S. Sharma, P. Redhu, Effect of multi-phase optimal velocity function on jamming transition in a lattice hydrodynamic model with passing, *Nonlinear Dynamics* 80 (2015) 1091–1108.
- [31] R. Jiang, Q. Wu, Z. Zhu, Full velocity difference model for a car-following theory, *Physical Review E* 64 (1) (2001) 017101.